Hindawi Publishing Corporation
Mathematical Problems in Engineering
Volume 2011, Article ID 927876, 28 pages
doi:10.1155/2011/927876

Research Article

Exact Solution for the Time-Dependent Temperature Field in Dry Grinding: Application to Segmental Wheels

J. L. González-Santander,[1] J. M. Valdés Placeres,[2] and J. M. Isidro[3]

[1] *Cátedra Energesis de Tecnología Interdisciplinar, Universidad Católica de Valencia, 46002 Valencia, Spain*
[2] *Departamento de Matemáticas, Universidad de Pinar del Río, 20200 Pinar del Río, Cuba*
[3] *Instituto Universitario de Matemática Pura y Aplicada, Universidad Politécnica de Valencia, 46022 Valencia, Spain*

Correspondence should be addressed to J. L. González-Santander, martinez.gonzalez@ucv.es

Received 21 February 2011; Accepted 1 April 2011

Academic Editor: Ezzat G. Bakhoum

We present a closed analytical solution for the time evolution of the temperature field in dry grinding for any time-dependent friction profile between the grinding wheel and the workpiece. We base our solution in the framework of the Samara-Valencia model Skuratov et al., 2007, solving the integral equation posed for the case of dry grinding. We apply our solution to segmental wheels that produce an intermittent friction over the workpiece surface. For the same grinding parameters, we plot the temperature fields of up- and downgrinding, showing that they are quite different from each other.

1. Introduction

A major technological challenge in the grinding of metallic plates [1–5] is how to avoid thermal damage to the workpiece. The grinding process transforms large amounts of mechanical energy into heat, which primarily affects the contact area between the workpiece and the wheel. It is therefore of great industrial importance to determine the temperature distribution within the workpiece, and its maximum, in order to avoid thermal damage.

Despite the fact that there have been studies of the temperature field solving the heat equation numerically [6, 7], an analytical approach is of great interest [8] for two reasons. Firstly, explicit expressions for the dependence of the temperature field with respect to the grinding parameters can be obtained. Secondly, the rapid presentation of results allows the industry to monitor the grinding process on line.

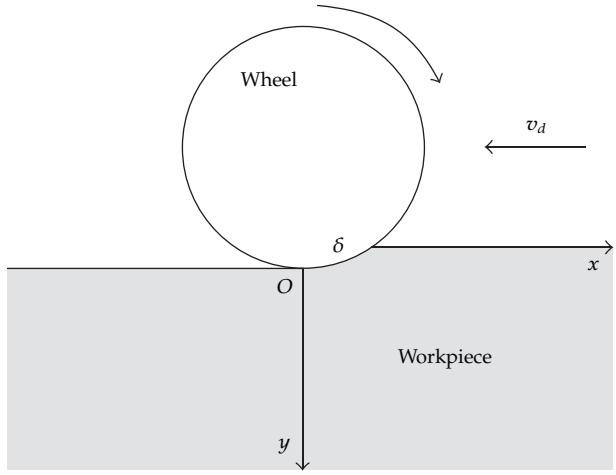

Figure 1: Bidimensional model for flat grinding.

This paper is organized as follows. Section 2 presents the Samara-Valencia model [9]. This model is used in Section 3 to derive a closed analytical solution for the evolution of the temperature field in dry grinding, for any time-dependent friction profile between the grinding wheel and the workpiece. Section 4 applies the result obtained in the previous section to intermittent grinding, for both up- and downgrindings. Section 5 analyzes some important variables in continuous grinding, such as the location of the maximum temperature and the relaxation time, which can be applied to intermittent grinding. We compare also the stationary regime of continuous grinding with the quasistationary regime of intermittent grinding. In Section 6, we present some numerical results, comparing continuous and intermittent grinding. Our conclusions are summarized in Section 7.

2. Samara-Valencia Model

The Samara-Valencia model setup is depicted in Figure 1. The workpiece moves at a constant speed v_d and is assumed to be infinite along Ox and Oz, and semiinfinte along Oy. The plane $y = 0$ is the surface being ground. The contact area between the wheel and the workpiece is an infinitely long strip of width δ located parallel to the Oz axis and on the plane $y = 0$. Both the wheel and the workpiece are assumed to be rigid. Although the equations below allow for the case of wet grinding, we will consider in this paper the case of dry grinding. The Samara-Valencia model [9] solves the convection heat equation

$$\partial_t T(t,x,y) = k\left[\partial_{xx} T(t,x,y) + \partial_{yy} T(t,x,y)\right] - v_d \partial_x T(t,x,y), \tag{2.1}$$

subject to the initial condition,

$$T(0,x,y) = 0, \tag{2.2}$$

and the boundary condition,

$$k_0 \partial_y T(t,x,0) = b(t,x)T(t,x,0) + d(t,x), \tag{2.3}$$

where $-\infty < x < \infty$ and $t, y \geq 0$. The first term of (2.3) models the application of coolant over the workpiece surface considering $b(t,x)$ as the heat transfer coefficient. The second term, $d(t,x)$, represents the heat flux entering into the workpiece. This heat flux is generated on the surface by friction between the wheel and the workpiece. The solution of the Samara-Valencia model (2.1)–(2.3) may be presented as the sum of two terms,

$$T(t,x,y) := T^{(0)}(t,x,y) + T^{(1)}(t,x,y), \tag{2.4}$$

where

$$T^{(0)}(t,x,y) := -\frac{1}{4\pi k_0} \int_0^t \frac{ds}{s} \exp\left(\frac{-y^2}{4ks}\right) \int_{-\infty}^{\infty} dx' d(t-s,x') \exp\left(-\frac{(x'-x-v_d s)^2}{4ks}\right), \tag{2.5}$$

$$\begin{aligned} T^{(1)}(t,x,y) := {} & \frac{1}{4\pi} \int_0^t \frac{ds}{s} \exp\left(\frac{-y^2}{4ks}\right) \int_{-\infty}^{\infty} dx' \left(\frac{y}{2ks} - \frac{b(t-s,x')}{k_0}\right) \\ & \times T(t-s,x',0) \exp\left(-\frac{(x'-x-v_d s)^2}{4ks}\right). \end{aligned} \tag{2.6}$$

Notice that $T^{(0)}$ contains the friction function $d(t,x)$, and $T^{(1)}$ contains the temperature field on the surface and the heat transfer coefficient $b(t,x)$.

3. $T^{(0)}$ Theorem for Dry Grinding

3.1. Dry Grinding

When no coolant is applied to the workpiece, we can consider the workpiece to be isolated from the environment. According to Newton's cooling law, this means that there is no heat flux from the workpiece to the environment, thus the heat transfer coefficient is zero,

$$b(t,x) = 0. \tag{3.1}$$

In this case of dry grinding, the expression for $T^{(1)}$ given in (2.6) becomes

$$\begin{aligned} T^{(1)}(t,x,y) = {} & \frac{y}{8\pi k} \int_0^t \exp\left(\frac{-y^2}{4ks}\right) \frac{ds}{s^2} \\ & \times \int_{-\infty}^{\infty} dx' \; T(t-s,x',0) \exp\left(-\frac{(x'-x-v_d s)^2}{4ks}\right). \end{aligned} \tag{3.2}$$

In order to tackle the integral equation given in (3.2), let us define the following integral operators

$$T^{(1)}(t,x,y) = \beth_y[T(t,x,0)], \tag{3.3}$$

where

$$\beth_y[T(t,x,0)] := \frac{y}{8\pi k}\int_0^t \frac{ds}{s^2}\exp\left(\frac{-y^2}{4ks}\right)\aleph_s[T(t,x,0)], \tag{3.4}$$

$$\aleph_s[T(t,x,0)] := \int_{-\infty}^{\infty} dx' T(t-s,x',0)\exp\left[-\frac{(x'-x-v_d s)^2}{4ks}\right]. \tag{3.5}$$

Therefore, taking into account (3.3), we may rewrite (2.4) as

$$T(t,x,y) = T^{(0)}(t,x,y) + \beth_y[T(t,x,0)]. \tag{3.6}$$

3.2. The $\aleph_s$ Operator

Let us calculate the $\aleph_s$ operator over the frictional term $T^{(0)}$ of the temperature field. According to (2.5), $T^{(0)}$ may be expressed as

$$T^{(0)}(t-s,x',0) = \frac{-1}{4\pi k_0}\int_0^{t-s}\frac{d\sigma}{\sigma}\int_{-\infty}^{\infty} d\xi d(t-s-\sigma,\xi)\exp\left(-\frac{(\xi-x'-v_d\sigma)^2}{4k\sigma}\right). \tag{3.7}$$

Therefore, substituting (3.7) in (3.5), and reordering the integrals by Fubini's theorem, we obtain

$$\begin{aligned}\aleph_s\left[T^{(0)}(t,x,0)\right] = \frac{-1}{4\pi k_0}&\int_{-\infty}^{\infty} d\xi \int_0^{t-s}\frac{d\sigma}{\sigma} d(t-s-\sigma,\xi)\\ &\times\int_{-\infty}^{\infty} dx' \exp\left(-\frac{(x'-x-v_d s)^2}{4ks}-\frac{(\xi-x'-v_d\sigma)^2}{4k\sigma}\right).\end{aligned} \tag{3.8}$$

Expanding the exponent of the integrand given in (3.8), we arrive at

$$\begin{aligned}\aleph_s\left[T^{(0)}(t,x,0)\right] &= \frac{-1}{4\pi k_0}\exp\left(-\frac{(x+v_d s)^2}{4ks}\right)\\ &\quad\times\int_{-\infty}^{\infty} d\xi \exp\left(\frac{v_d\xi}{2k}\right)\\ &\quad\times\int_0^{t-s}\frac{d\sigma}{\sigma}d(t-s-\sigma,\xi)\exp\left(-\frac{\xi^2}{4k\sigma}-\frac{v_d^2\sigma}{4k}\right)\\ &\quad\times\int_{-\infty}^{\infty} dx' \exp\left[-\frac{x'^2}{4k}\left(\frac{s+\sigma}{s\sigma}\right)+\frac{x'}{2k}\left(\frac{x\sigma+\xi s}{s\sigma}\right)\right].\end{aligned} \tag{3.9}$$

The last integral given in (3.9) can be calculated [10, Equation 3.323.2], so that,

$$\begin{aligned}\aleph_s\left[T^{(0)}(t,x,0)\right] &= \frac{-\sqrt{ks}}{2\sqrt{\pi}k_0}\exp\left(-\frac{(x+v_d s)^2}{4ks}\right)\\ &\quad\times\int_{-\infty}^{\infty} d\xi \exp\left(\frac{v_d\xi}{2k}\right)\\ &\quad\times\int_0^{t-s} d\sigma\frac{d(t-s-\sigma,\xi)}{\sqrt{\sigma}\sqrt{s+\sigma}}\exp\left(\frac{(x\sigma+\xi s)^2}{4ks\sigma(s+\sigma)}-\frac{\xi^2}{4k\sigma}-\frac{v_d^2\sigma}{4k}\right).\end{aligned} \tag{3.10}$$

Once again, expanding the exponent of the last integrand given in (3.10) and simplifying, we arrive at

$$\begin{aligned}\aleph_s\left[T^{(0)}(t,x,0)\right] &= \frac{-\sqrt{ks}}{2\sqrt{\pi}k_0}\exp\left(-\frac{xv_d}{2k}\right)\int_{-\infty}^{\infty} d\xi \exp\left(\frac{v_d\xi}{2k}\right)\\ &\quad\times\int_0^{t-s} d\sigma\frac{d(t-s-\sigma,\xi)}{\sqrt{\sigma}\sqrt{s+\sigma}}\exp\left(-\frac{(x-\xi)^2}{4k(s+\sigma)}-\frac{v_d^2}{4k}(\sigma+s)\right).\end{aligned} \tag{3.11}$$

Let us define

$$I_\sigma := \int_0^{t-s} d\sigma\frac{d(t-s-\sigma,\xi)}{\sqrt{\sigma}\sqrt{s+\sigma}}\exp\left(-\frac{(x-\xi)^2}{4k(s+\sigma)}-\frac{v_d^2}{4k}(\sigma+s)\right). \tag{3.12}$$

We can calculate (3.12) performing the substitution, $\mu = \sigma + s$, and introducing the Heaviside function $H(x)$, so that,

$$I_\sigma = \int_0^t d\mu\frac{d(t-\mu,\xi)}{\sqrt{\mu-s}\sqrt{\mu}}\exp\left(-\frac{(x-\xi)^2}{4k\mu}-\frac{v_d^2}{4k}\mu\right)H(\mu-s). \tag{3.13}$$

Substituting (3.13) in (3.11) and simplifying, we get

$$\aleph_s\left[T^{(0)}(t,x,0)\right] = \frac{-\sqrt{ks}}{2\sqrt{\pi}k_0}\int_{-\infty}^{\infty} d\xi \int_0^t d\mu \frac{d(t-\mu,\xi)}{\sqrt{\mu-s}\sqrt{\mu}} \exp\left(-\frac{(\xi-x-v_d\mu)^2}{4k\mu}\right) H(\mu-s). \tag{3.14}$$

3.3. The $\beth_y$ Operator

Substituting the expression obtained in (3.14) into (3.4) and reordering the integrals, we have

$$\begin{aligned}\beth_y\left[T^{(0)}(t,x,0)\right] = {} & \frac{-y}{16\pi^{3/2}k_0\sqrt{k}}\int_{-\infty}^{\infty} d\xi \\ & \times \int_0^t d\mu \frac{d(t-\mu,\xi)}{\sqrt{\mu}} \exp\left(-\frac{(\xi-x-v_d\mu)^2}{4k\mu}\right) \\ & \times \int_0^t ds \frac{H(\mu-s)}{s^{3/2}\sqrt{\mu-s}} \exp\left(\frac{-y^2}{4ks}\right).\end{aligned} \tag{3.15}$$

Let us define

$$I_s := \int_0^t ds \frac{H(\mu-s)}{s^{3/2}\sqrt{\mu-s}} \exp\left(\frac{-y^2}{4ks}\right). \tag{3.16}$$

Since $\mu \in [0,t]$, the integral given in (3.16) can be expressed in the following way:

$$I_s = \int_0^{\mu} \frac{ds}{s^{3/2}\sqrt{\mu-s}} \exp\left(\frac{-y^2}{4ks}\right). \tag{3.17}$$

In order to calculate (3.17), we can perform the following substitutions: $s = \mu/t$, $w = \sqrt{t-1}$ and $r = yw/2\sqrt{k\mu}$, leading to

$$I_s = \frac{2\sqrt{\pi k}}{y\sqrt{\mu}} \exp\left(-\frac{y^2}{4k\mu}\right). \tag{3.18}$$

Therefore, substituting (3.18) in (3.15) and changing the integration order, we arrive at

$$\beth_y\left[T^{(0)}(t,x,0)\right] = \frac{-1}{8\pi k_0}\int_0^t \frac{d\mu}{\mu} \exp\left(-\frac{y^2}{4k\mu}\right) \int_{-\infty}^{\infty} d\xi\, d(t-\mu,\xi) \exp\left(-\frac{(x-\xi-v_d\mu)^2}{4k\mu}\right). \tag{3.19}$$

Remembering the expression for $T^{(0)}$ given in (2.5), we conclude

$$\beth_y\left[T^{(0)}(t,x,0)\right] = \frac{1}{2}T^{(0)}(t,x,y). \tag{3.20}$$

3.4. Resolution by Successive Approximations

According to (3.2), in order to evaluate $T^{(1)}$, we have to know the temperature field on the surface, $T(t,x,0)$. At zeroth order approximation, T_0, we can consider that the temperature field will be given by the term involving friction only, that is, $T^{(0)}$ according to (2.5). So that,

$$T_0(t,x,y) = T^{(0)}(t,x,y). \tag{3.21}$$

In order to get the first-order approximation T_1, we can substitute the zeroth order (3.21) in (3.3),

$$T_1^{(1)}(t,x,y) = \beth_y[T_0(t,x,0)] = \beth_y\left[T^{(0)}(t,x,0)\right]. \tag{3.22}$$

Thus, the temperature field at first order is

$$T_1(t,x,y) = T^{(0)}(t,x,y) + T_1^{(1)}(t,x,y), \tag{3.23}$$

or according to (3.22),

$$T_1(t,x,y) = T^{(0)}(t,x,y) + \beth_y[T_0(t,x,0)]. \tag{3.24}$$

In general, the nth ($n = 0,1,2,\ldots$) approximation is

$$T_n(t,x,y) := T^{(0)}(t,x,y) + \beth_y[T_{n-1}(t,x,0)], \tag{3.25}$$

where the initial value is given by (3.21). Applying now (3.20) to (3.22), we can rewrite the first-order approximation as

$$T_1(t,x,y) = \frac{3}{2}T^{(0)}(t,x,y). \tag{3.26}$$

In order to evaluate the second order, we can substitute (3.26) in the recurrence equation (3.25) for $n = 2$. Taking into account that the integral operator $\beth_y$ is linear, we obtain

$$\begin{aligned} T_2(t,x,y) &= T^{(0)}(t,x,y) + \beth_y[T_1(t,x,0)] \\ &= T^{(0)}(t,x,y) + \frac{3}{2}\beth_y\left[T^{(0)}(t,x,0)\right] \\ &= \frac{7}{4}T^{(0)}(t,x,y), \end{aligned} \tag{3.27}$$

where we have applied (3.20) once again. Repeating the same steps, we get at third order

$$T_3(t,x,y) = \frac{15}{8}T^{(0)}(t,x,y). \tag{3.28}$$

Looking at the coefficients appearing in the first orders, (3.26), (3.27), and (3.28), we may establish the following conjecture for the nth order:

$$T_n(t,x,y) = \frac{2^{n+1}-1}{2^n}T^{(0)}(t,x,y), \tag{3.29}$$

that can be proved by induction,

$$\begin{aligned} T_{n+1}(t,x,y) &= T^{(0)}(t,x,y) + \beth_y[T_n(t,x,0)] \\ &= T^{(0)}(t,x,y) + \frac{2^{n+1}-1}{2^n}\beth_y\left[T^{(0)}(t,x,0)\right] \\ &= \frac{2^{n+2}-1}{2^{n+1}}T^{(0)}(t,x,y). \end{aligned} \tag{3.30}$$

The temperature field will be the infinite order approximation, thus taking the limit of (3.29), results in

$$T(t,x,y) = \lim_{n\to\infty} T_n(t,x,y) = 2T^{(0)}(t,x,y). \tag{3.31}$$

Applying (3.20), we may check that (3.31) is a solution of the integral equation given in (3.6),

$$\begin{aligned} T(t,x,y) &= T^{(0)}(t,x,y) + \beth_y[T(t,x,0)] \\ &= T^{(0)}(t,x,y) + 2\beth_y\left[T^{(0)}(t,x,0)\right] \\ &= 2T^{(0)}(t,x,y). \end{aligned} \tag{3.32}$$

Taking into account (2.5), we conclude that the time evolution of the temperature field may be expressed as

$$T(t,x,y) = -\frac{1}{2\pi k_0}\int_0^t \frac{ds}{s}\exp\left(\frac{-y^2}{4ks}\right)\int_{-\infty}^{\infty} dx' d(t-s,x')\exp\left(-\frac{(x'-x-v_d s)^2}{4ks}\right). \tag{3.33}$$

3.5. Uniqueness of the Solution

3.5.1. Bound Limit for $\beth_0$

To prove the uniqueness of the solution of the integral equation (3.6), let us calculate first the value of the $\beth_y$ operator over a constant. According to (3.5), we have

$$\aleph_s[1] = \int_{-\infty}^{\infty} \exp\left[-\frac{(x' - x - v_d s)^2}{4ks}\right] dx'. \tag{3.34}$$

Performing the substitution: $u = (x' - x - v_d s)/2\sqrt{ks}$, (3.33) results in

$$\aleph_s[1] = 2\sqrt{ks}\int_{-\infty}^{\infty} e^{-u^2} du = 2\sqrt{\pi ks}. \tag{3.35}$$

Applying (3.35) to (3.4), we have

$$\beth_y[1] = \frac{y}{4\sqrt{\pi k}}\int_0^t \frac{ds}{s^{3/2}} \exp\left(\frac{-y^2}{4ks}\right). \tag{3.36}$$

Performing the substitution: $u = y/2\sqrt{ks}$, we have

$$\beth_y[1] = \frac{1}{\sqrt{\pi}}\int_{y/2\sqrt{kt}}^{\infty} e^{-u^2} du = \frac{1}{2}\operatorname{erfc}\left(\frac{y}{2\sqrt{kt}}\right). \tag{3.37}$$

Therefore,

$$\beth_0[1] = \frac{1}{2}. \tag{3.38}$$

Let us consider now a function $f(t, x, y)$ whose maximum value taking $y = 0$ is $f_{\max}$, that is,

$$f(t, x, 0) \leq f_{\max}. \tag{3.39}$$

Applying $\beth_0$ to (3.39) and taking into account that $\beth_0$ is a linear operator,

$$\beth_0\left[f(t, x, 0)\right] \leq \beth_0\left[f_{\max}\right] = f_{\max}\beth_0[1]. \tag{3.40}$$

Thus, according to (3.38),

$$\beth_0\left[f(t, x, 0)\right] \leq \frac{f_{\max}}{2}. \tag{3.41}$$

Note that, if we apply $\beth_0$ to (3.39) and we take into account (3.37), we have

$$\beth_0^{(2)}\left[f(t,x,0)\right] \leq \beth_0\left[\frac{f_{\max}}{2}\right] = \frac{f_{\max}}{2^2}. \tag{3.42}$$

So, in general, for all $n \in \mathbb{N}$,

$$\beth_0^{(n)}\left[f(t,x,0)\right] \leq \frac{f_{\max}}{2^n}. \tag{3.43}$$

3.5.2. Resolution of the Uniqueness

If $T_A(t,x,y)$ and $T_B(t,x,y)$ are solutions of (3.6), we have

$$T_A(t,x,y) = T^{(0)}(t,x,y) + \beth_y[T_A(t,x,0)], \tag{3.44}$$

$$T_B(t,x,y) = T^{(0)}(t,x,y) + \beth_y[T_B(t,x,0)]. \tag{3.45}$$

Subtracting (3.45) from (3.44) and taking into account that $\beth_y$ is a linear operator,

$$T_A(t,x,y) - T_B(t,x,y) = \beth_y[T_A(t,x,0) - T_B(t,x,0)]. \tag{3.46}$$

Taking $y = 0$ in (3.46),

$$T_A(t,x,0) - T_B(t,x,0) = \beth_0[T_A(t,x,0) - T_B(t,x,0)]. \tag{3.47}$$

Recursive substitution of (3.47) yields

$$T_A(t,x,0) - T_B(t,x,0) = \beth_0^{(n)}[T_A(t,x,0) - T_B(t,x,0)]. \tag{3.48}$$

If we take in (3.43) as a function f,

$$f_1(t,x,0) = T_A(t,x,0) - T_B(t,x,0), \tag{3.49}$$

according to (3.48), we have that, for all $n \in \mathbb{N}$,

$$T_A(t,x,0) - T_B(t,x,0) \leq \frac{f_{1,\max}}{2^n}, \tag{3.50}$$

where $f_{1,\max}$ is the maximum value of $f_1(t,x,0)$. Taking the limit in (3.50),

$$T_A(t,x,0) - T_B(t,x,0) \leq \lim_{n\to\infty} \frac{f_{1,\max}}{2^n} = 0, \tag{3.51}$$

so that,

$$T_A(t,x,0) \leq T_B(t,x,0). \tag{3.52}$$

Note that in (3.48) we can exchange labels A and B,

$$T_B(t,x,0) - T_A(t,x,0) = \beth_0^{(n)}[T_B(t,x,0) - T_A(t,x,0)]. \tag{3.53}$$

Thus, taking now the function

$$f_2(t,x,0) = T_B(t,x,0) - T_A(t,x,0), \tag{3.54}$$

we obtain that

$$T_B(t,x,0) - T_A(t,x,0) \leq \lim_{n\to\infty} \frac{f_{2,\max}}{2^n} = 0, \tag{3.55}$$

that is,

$$T_B(t,x,0) \leq T_A(t,x,0). \tag{3.56}$$

From (3.52) and (3.56), we conclude that both solutions on the surface are equal,

$$T_A(t,x,0) = T_B(t,x,0). \tag{3.57}$$

Applying $\beth_y$ to (3.57),

$$\beth_y[T_A(t,x,0)] = \beth_y[T_B(t,x,0)], \tag{3.58}$$

and substituting (3.58) in (3.44), we have that

$$T_A(t,x,y) = T^{(0)}(t,x,y) + \beth_y[T_B(t,x,0)]. \tag{3.59}$$

Comparing (3.45) with (3.59), we finally obtain

$$T_A(t,x,y) = T_B(t,x,y). \tag{3.60}$$

Therefore, the solution given in (3.33) is the only solution of (3.6).

4. Intermittent Grinding

Equation (3.31) is a generalization of the result presented in [11] since now the transient regime is considered and any type of time-dependent friction profile is allowed. In the next section, we will apply (3.31) to calculate the time-dependent temperature field produced by an intermittent grinding of a segmental wheel (Figure 2).

Figure 2: Profile of a toothed wheel.

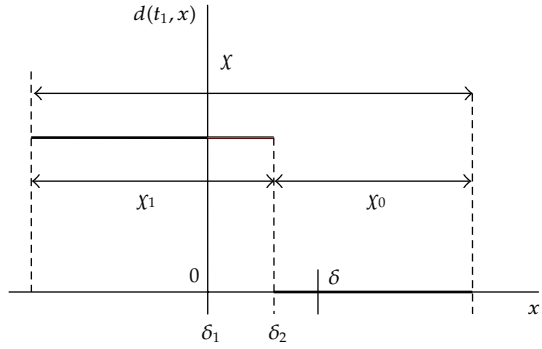

Figure 3: Friction function $d(t, x)$ for time t_1 highlighted in red.

4.1. Intermittence Function

Let us model the friction due to a toothed wheel, which can contact the workpiece within $x \in [0, \delta]$. Therefore, we will call this zone, *contact zone*. Figures 3 and 4 show the *friction zone* highlighted in red within the limits a and b for two different times t_1 and $t_2 > t_1$. The wheel has a spatial period $\chi = \chi_0 + \chi_1$, where χ_0 is the distance between teeth and χ_1 is the tooth width. The wheel teeth move at a speed $v_m = \omega R$, where ω is the angular velocity and R is the wheel radius. When more than two teeth touch simultaneously the contact zone $[0, \delta]$, the friction zone is split as Figure 5 shows. For a given instant t, the incoming heat flux $d(t, x)$ enters the workpiece through the friction zone: $x \in (a_j, b_j)$, $j = 0, \ldots, n + 1$, where j indicates a wheel tooth. Notice that there can be up to $n + 2$ teeth within the contact zone, where

$$n := \left\lfloor \frac{\delta}{\chi} \right\rfloor. \tag{4.1}$$

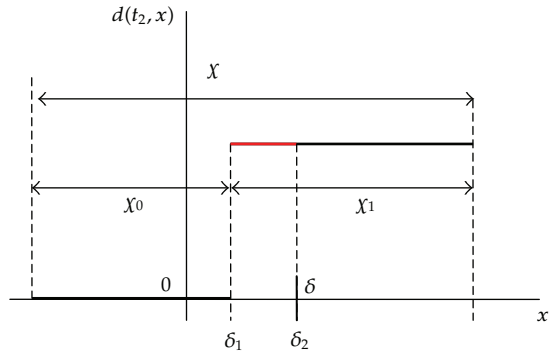

Figure 4: Friction function $d(t, x)$ for time $t_2 > t_1$ highlighted in red.

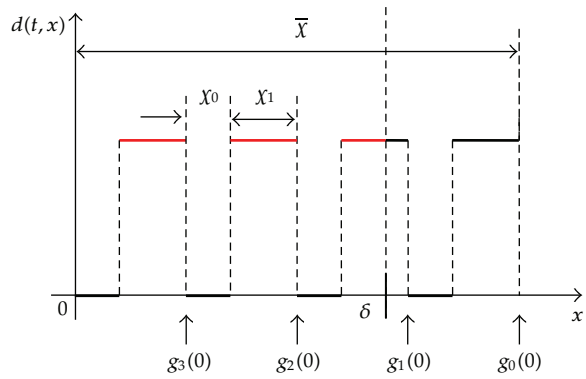

Figure 5: Initial location of the $g_j(t)$ points, for $n = 2$.

Note, also, that the friction limits are time dependent: $a_j = a_j(t)$ and $b_j = b_j(t)$. If the incoming heat flux q is constant for every point where friction occurs, we may write the friction function as

$$d(t, x) = -q \sum_{j=0}^{n+1} H\left(x - a_j(t)\right) H\left(b_j(t) - x\right), \tag{4.2}$$

where $H(x)$ is the Heaviside function. In order to know the friction limits of the wheel teeth $(j = 0, \ldots, n + 1)$ which enters into the contact zone, that is, a_j and b_j, let us define the spatial period,

$$\overline{\chi} := (n + 2)\chi. \tag{4.3}$$

According to Figure 5, the $g_j(t)$ points, $j = 0, \ldots, n + 1$, are initially over the period $\overline{\chi}$,

$$g_j(t) := (-1)^{\phi} v_m t + \overline{\chi} - j\chi, \tag{4.4}$$

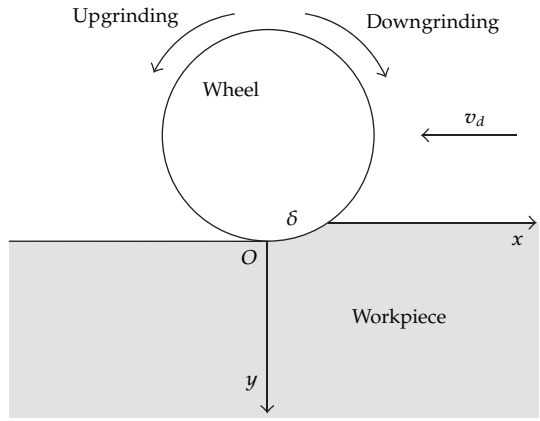

Figure 6: Upgrinding and downgrinding according to the wheel rotation.

where we have defined a boolean variable ϕ, in order to define the rotation of the wheel: $\phi = 1$, downgrinding; $\phi = 0$, upgrinding, as Figure 6 shows. If we want a periodic repetition of the friction limits over the period $\overline{\chi}$, we may define the function

$$f_j(t) = g_j(t) - \left\lfloor \frac{g_j(t)}{\overline{\chi}} \right\rfloor \overline{\chi}. \tag{4.5}$$

We want as well that $b_j \in [0, \delta]$, thus,

$$b_j(t) = \min\left[\max\left(f_j(t), 0\right), \delta\right] = \begin{cases} b_j(t) & 0 < b_j(t) < \delta, \\ 0 & b_j(t) \leq 0, \\ \delta & b_j(t) \geq \delta. \end{cases} \tag{4.6}$$

Similarly, since the tooth width is χ_1,

$$a_j(t) = \min\left[\max\left(f_j(t) - \chi_1, 0\right), \delta\right]. \tag{4.7}$$

The min and max functions are given by

$$\begin{aligned} \min(a, b) &= \frac{a + b - |a - b|}{2}, \\ \max(a, b) &= \frac{a + b + |a - b|}{2}. \end{aligned} \tag{4.8}$$

4.2. Temperature Field

Substituting (4.2) in (3.33), we obtain

$$T(t,x,y) = \frac{q}{2\pi k_0}\int_0^t \frac{ds}{s}\exp\left(\frac{-y^2}{4ks}\right) \times \sum_{j=0}^{n+1}\int_{a_j(t-s)}^{b_j(t-s)} dx' \exp\left(-\frac{(x'-x-v_d s)^2}{4ks}\right). \tag{4.9}$$

Let us evaluate the integral over the x' variable in (4.9),

$$I_{x'} := \sum_{j=0}^{n+1}\int_{a_j(t-s)}^{b_j(t-s)} \exp\left(-\frac{(x'-x-v_d s)^2}{4ks}\right) dx'. \tag{4.10}$$

Performing the substitution,

$$u = \frac{x'-x-v_d s}{2\sqrt{ks}}, \tag{4.11}$$

and taking into account the properties of the error function, we get

$$I_{x'} = \sqrt{\pi k s}\ \mathrm{ERF}(t,x,s), \tag{4.12}$$

where we have defined the function

$$\mathrm{ERF}(t,x,s) := \sum_{j=0}^{n+1}\mathrm{erf}\left(\frac{x+v_d s-a_j(t-s)}{2\sqrt{ks}}\right) - \mathrm{erf}\left(\frac{v_d s+x-b_j(t-s)}{2\sqrt{ks}}\right). \tag{4.13}$$

Substituting (4.12) in (4.9), we obtain the following expression for the temperature field:

$$T(t,x,y) = \frac{q\sqrt{k}}{2\sqrt{\pi}k_0}\int_0^t \frac{ds}{\sqrt{s}}\exp\left(\frac{-y^2}{4ks}\right)\mathrm{ERF}(t,x,s). \tag{4.14}$$

5. Continuous Grinding

5.1. Stationary Regime

In order to calculate the temperature field for the case of continuous friction, we can take in (4.7)-(4.6) the constant values of the contact zone,

$$\begin{aligned} a_0(t) &= 0, \\ b_0(t) &= \delta. \end{aligned} \tag{5.1}$$

Therefore, we can redefine (4.12) as

$$\mathrm{ERF}_{\mathrm{cont}}(x,s) := \mathrm{erf}\left(\frac{x+v_d s}{2\sqrt{ks}}\right) - \mathrm{erf}\left(\frac{v_d s + x - \delta}{2\sqrt{ks}}\right), \tag{5.2}$$

obtaining, according to (4.13), the following temperature field:

$$T_{\mathrm{cont}}(t,x,y) = \frac{q\sqrt{k}}{2\sqrt{\pi}k_0}\int_0^t \frac{ds}{\sqrt{s}}\exp\left(\frac{-y^2}{4ks}\right)\mathrm{ERF}_{\mathrm{cont}}(x,s). \tag{5.3}$$

The stationary regime is reached when the temperature field does not vary in time,

$$\frac{\partial T}{\partial t} = 0. \tag{5.4}$$

In the case of continuous grinding, the time derivative is

$$\frac{\partial T_{\mathrm{cont}}(t,x,y)}{\partial t} = \frac{q\sqrt{k}}{2k_0}\frac{\mathrm{ERF}_{\mathrm{cont}}(x,t)}{\sqrt{\pi t}}\exp\left(\frac{-y^2}{4kt}\right). \tag{5.5}$$

Taking the limit of (5.4), knowing that $\mathrm{erf}(\pm\infty) = \pm 1$, we can check that the stationary regime is reached when $t \to \infty$:

$$\lim_{t\to\infty}\mathrm{ERF}_{\mathrm{cont}}(x,t) = \lim_{t\to\infty}\mathrm{erf}\left(\frac{x+v_d t}{2\sqrt{kt}}\right) - \mathrm{erf}\left(\frac{v_d t + x - \delta}{2\sqrt{kt}}\right) = 0, \tag{5.6}$$

so that,

$$\lim_{t\to\infty}\frac{\partial T_{\mathrm{cont}}(t,x,y)}{\partial t} = 0. \tag{5.7}$$

5.2. Quasistationary Regime

Notice that intermittent grinding never reaches a stationary regime, since the heat source produced by friction is pulsed. This is not the case of continuous grinding, where the stationary regime is reached asymptotically for $t \to \infty$. Therefore, for continuous grinding, we may define a relaxation time t^* that provides us an idea of how rapid the stationary regime is reached in practice. It turns out that this relaxation time, defined for the continuous case, is a good temporal reference in order to plot the temperature field in the case of intermittent grinding. Even though intermittent grinding never reaches a stationary regime, we may define a quasistationary regime in which the temperature field is periodically stable. Since $a_j(t)$ and $b_j(t)$ are periodic functions (4.6)-(4.7), according to (4.14), we may define the quasistationary regime as

$$T_\infty(t,x,y) := \frac{q\sqrt{k}}{2\sqrt{\pi}k_0}\int_0^\infty \frac{ds}{\sqrt{s}}\exp\left(\frac{-y^2}{4ks}\right)\mathrm{ERF}(t,x,s). \tag{5.8}$$

According to Figure 5, the temporal period of the friction function $d(t, x_0)$ in a fixed point $x = x_0$ is

$$\tau := \frac{\chi}{v_m}. \tag{5.9}$$

However, the global consideration of the $d(t, x)$ plot indicates the following temporal period:

$$\overline{\tau} := \frac{\overline{\chi}}{v_m}. \tag{5.10}$$

In view of (3.31), we may conclude that $T_\infty(t, x, y)$ possesses the same global and point periods τ and $\overline{\tau}$ as the friction function $d(t, x)$.

5.3. Maximum Temperature

Since the error function $\mathrm{erf}(z)$ is an increasing function for all z, we have

$$\mathrm{ERF}_{\mathrm{cont}}(x, t) > 0 \quad t > 0,\ x \in \mathbb{R}. \tag{5.11}$$

Therefore, the temperature on a given point (x, y) of the workpiece is a monotonically increasing function,

$$\frac{\partial T_{\mathrm{cont}}(t, x, y)}{\partial t} > 0 \quad y, t > 0,\ x \in \mathbb{R}. \tag{5.12}$$

Equation (5.12) means that the maximum temperature must be reached in the stationary state, $t \to \infty$. Moreover, as in (5.11), we have

$$\mathrm{ERF}_{\mathrm{cont}}(x, s) > 0 \quad s \in (0, t),\ x \in \mathbb{R}, \tag{5.13}$$

so that, for $y > 0$,

$$\frac{\partial T_{\mathrm{cont}}(t, x, y)}{\partial y} = -\frac{qy}{4\sqrt{\pi k}k_0} \int_0^t \frac{ds}{s^{3/2}} \exp\left(\frac{-y^2}{4ks}\right) \mathrm{ERF}_{\mathrm{cont}}(x, s) < 0. \tag{5.14}$$

Equation (5.14) indicates that maximum temperature must be localized on the surface, $y = 0$. From (5.12) and (5.14), we conclude that the maximum temperature must be reached on the surface in the stationary regime,

$$T_{\max} = \lim_{t \to \infty} T_{\mathrm{cont}}(t, x_{\max}, 0). \tag{5.15}$$

This result agrees with [11].

5.3.1. Location of the Maximum Temperature

Denoting the stationary regime in the case of continuous friction as

$$T_{\text{cont}}(x,y) := \lim_{t\to\infty} T_{\text{cont}}(t,x,y), \tag{5.16}$$

according to [12], we have,

$$T_{\text{cont}}(X,Y) = \tau \int_{-X}^{\Delta-X} e^{u} K_0\left(\sqrt{u^2+Y^2}\right)\, du, \tag{5.17}$$

where K_0 is the modified Bessel function of zeroth order [13, Section 9.6.], X and Y are spatial dimensionless coordinates, and τ is a characteristic temperature,

$$\begin{aligned} \zeta &:= \frac{v_d}{2k}, \\ \tau &:= \frac{q}{2\pi k_0 \zeta}, \\ Y &:= \zeta y, \\ X &:= \zeta x, \\ \Delta &:= \zeta \delta. \end{aligned} \tag{5.18}$$

According to what we have seen in (5.15), the maximum temperature is reached on the surface at the stationary regime. Thus, we have to analyze the maximum of the function given in (5.17) taking $Y = 0$, that is,

$$T_{\text{cont}}(X,0) = \tau \int_{-X}^{\Delta-X} e^{u} K_0(|u|)\, du. \tag{5.19}$$

In order to determine the location of the maximum on the surface, firstly let us calculate the points X_m where $T_{\text{cont}}(X,0)$ has a null derivative (extrema points),

$$\left.\frac{dT_{\text{cont}}(X,0)}{dX}\right|_{X=X_m} = \tau\left[e^{-X_m} K_0(|X_m|) - e^{\Delta-X_m} K_0(|\Delta - X_m|)\right] = 0. \tag{5.20}$$

Therefore, X_m satisfies

$$g(X_m) = e^{\Delta}, \tag{5.21}$$

where

$$g(X) := \frac{K_0(|X|)}{K_0(|\Delta - X|)}. \tag{5.22}$$

When $v_d > 0$, the workpiece moves as indicates Figure 1, so that, now on we will consider $\Delta > 0$. Since the incoming heat flux into the workpiece is a positive magnitude, $q > 0$, we have, $\tau > 0$. Moreover, since K_0 is positive for positive arguments [13, Section 9.6.], the integrand of (5.21) is also positive, thus,

$$T_{\text{cont}}(X, 0) > 0. \tag{5.23}$$

Location of the Extrema

Assume first that $X_m > \Delta > 0$, so that (5.19) results in

$$\frac{K_0(X_m)}{K_0(X_m - \Delta)} = e^{\Delta}. \tag{5.24}$$

We may rewrite (5.24) as $h_1(\Delta) = h_1(0)$, where $h_1(\Delta) := e^{\Delta} K_0(X_m - \Delta)$. Since K_0 is positive for positive arguments [13, Section 9.6.], we have for all $X_m > \Delta > 0$,

$$h_1'(\Delta) = e^{\Delta}[K_1(X_m - \Delta) + K_0(X_m - \Delta)] > 0, \tag{5.25}$$

that is, $h_1(\Delta) > h_1(0)$, for $X_m > \Delta > 0$. Therefore, we conclude

$$X_m \notin (\Delta, \infty). \tag{5.26}$$

Assume now that $X_m < 0$, so that (5.21) becomes

$$\frac{K_0(-X_m)}{K_0(\Delta - X_m)} = e^{\Delta}. \tag{5.27}$$

Performing the change of variables $Z = -X_m > 0$, (5.27) is equivalent to $h_2(\Delta) = h_2(0)$, where $h_2(\Delta) := e^{\Delta} K_0(\Delta + Z)$. Due to the integral representation [13, Equation 9.6.24],

$$K_\nu(z) = \int_0^\infty \exp[-z \cosh \alpha] \cosh \nu\alpha \, d\alpha, \tag{5.28}$$

and since for all $\alpha > 0$, $\cosh \alpha > 1$, we have for all $Z, \Delta > 0$,

$$h_2'(\Delta) = e^{\Delta}[K_0(\Delta + Z) - K_1(\Delta + Z)] < 0. \tag{5.29}$$

So that, $h_2(\Delta) < h_2(0)$, for $Z, \Delta > 0$. That is, (5.27) is not satisfied for $X_m < 0$,

$$X_m \notin (-\infty, 0). \tag{5.30}$$

Finally, assume that $X \in (0, \Delta)$, so that $|X| = X$ and $|\Delta - X| = \Delta - X$, and therefore, according to (5.22),

$$g(X) = \frac{K_0(X)}{K_0(\Delta - X)}, \quad X \in (0, \Delta). \tag{5.31}$$

Since $g(X)$ is a continuous function in $X \in (0, \Delta)$ and,

$$\begin{aligned} \lim_{X \to 0} g(X) &= +\infty, \\ \lim_{X \to \Delta} g(X) &= 0, \end{aligned} \tag{5.32}$$

according to Bolzano's theorem,

$$\exists X_m \in (0, \Delta) \quad \text{so that } g(X_m) = e^{\Delta}. \tag{5.33}$$

Uniqueness of the Extremum and Identification as Maximum

Since K_0 is a positive and monotonically decreasing function for positive arguments, $K_0(x) > 0$, $K_0'(x) < 0$ for $x > 0$, [13, Section 9.6.] we have that $g(X)$ is a monotonically decreasing function for $X \in (0, \Delta)$,

$$g'(X) = \frac{K_0'(X)K_0(\Delta - X) + K_0(X)K_0'(\Delta - X)}{K_0^2(\Delta - X)} < 0. \tag{5.34}$$

Therefore, according to (5.33),

$$\exists! X_m \in (0, \Delta) \quad \text{so that } g(X_m) = e^{\Delta}. \tag{5.35}$$

On the one hand, according to (5.26), (5.30), and (5.35), $T_{\text{cont}}(X, 0)$ has a unique extremum in X_m and this one always occurs within the interval $X_m \in (0, \Delta)$. On the other hand, from (5.19) we can see that

$$\lim_{X \to \pm\infty} T_{\text{cont}}(X, 0) = \lim_{X \to \pm\infty} \tau \int_{-X}^{\Delta - X} e^u K_0(|u|) du = 0. \tag{5.36}$$

Since $T_{\text{cont}}(X, 0)$ is a positive (5.23), continuous and differentiable function, which satisfies (5.36), the only possibility is that the extremum X_m corresponds to a global maximum. Therefore, just compute a root X_m of (5.21) within the interval $X \in (0, \Delta)$, that is taking (5.31), in order to get the location on the surface of the maximum temperature,

$$x_{\max} = \frac{X_m}{\zeta}. \tag{5.37}$$

There is an equivalent, but more elaborated proof, in [14].

5.4. Relaxation Time

In order to estimate how rapid the transient regime is, according to (5.4), we will be close to it when, for a certain time $\bar{t}$,

$$\frac{\partial T_{\text{cont}}\left(\bar{t}, x, y\right)}{\partial t} = \epsilon \approx 0 \tag{5.38}$$

is satisfied. Notice that (5.38) depends on the workpiece point (x, y) chosen for the evaluation of $\bar{t}$. We can define the relaxation time t^*, as the time that satisfies (5.38) over the maximum temperature point. According to (5.15), that point must be on the surface in the stationary state, $(x, y) = (x_{\max}, 0)$, thus,

$$\frac{\partial T_{\text{cont}}(t^*, x_{\max}, 0)}{\partial t} = \frac{q\sqrt{k}}{2k_0} \frac{\text{ERF}(x_{\max}, t^*)}{\sqrt{\pi t^*}} = \epsilon. \tag{5.39}$$

Equation (5.39) can be solved numerically. In order to solve it approximately, we can expand the following function up to the first order, near the stationary regime $t \to \infty$, [13, Equation 7.1.6]:

$$h(t, z) := \text{erf}\left(\frac{v_d}{2\sqrt{k}}\sqrt{t} + \frac{z}{2\sqrt{kt}}\right) \underset{t\to\infty}{\sim} \text{erf}\left(\frac{v_d}{2\sqrt{k}}\sqrt{t}\right) + \frac{z}{\sqrt{\pi kt}} \exp\left(-\frac{v_d^2 t}{4k}\right). \tag{5.40}$$

Therefore,

$$\text{ERF}(x, t) = h(t, x) - h(t, x - \delta) \underset{t\to\infty}{\sim} \frac{\delta}{\sqrt{\pi kt}} \exp\left(-\frac{v_d^2 t}{4k}\right). \tag{5.41}$$

Substituting (5.41) in (5.39), we have the following approximated equation:

$$\frac{q\delta}{2\pi k_0 t^*} \exp\left(-\frac{v_d^2 t^*}{4k}\right) \approx \epsilon. \tag{5.42}$$

Using the Lambert function W [15], we can derive the relaxation time from (5.42), arriving at,

$$t^* \approx \frac{4k}{v_d^2} W\left(\frac{q\delta v_d^2}{8\pi k k_0 \epsilon}\right). \tag{5.43}$$

Notice that in (5.43), the relaxation time is independent of the localization of the maximum on the surface $x_{\max}$, thus it can be computed much more rapidly.

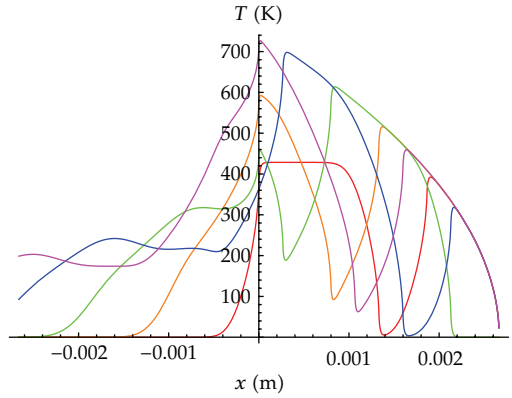

Figure 7: Surface temperature evolution in continuous grinding $T_{\text{cont}}(t, x, 0)$ for $x \in (-\delta, \delta)$ and $t = t^* m/5$, taking $m = 1, 2, 3, 4, 5$ (red, orange, green, blue, magenta, resp.).

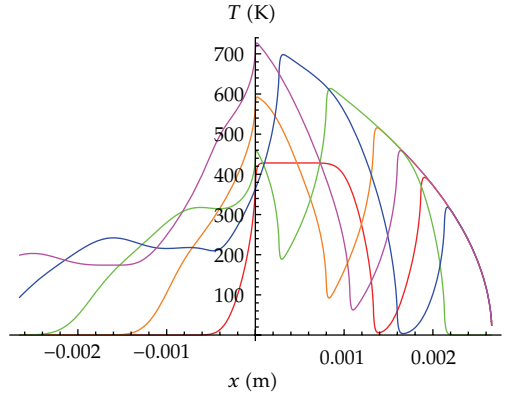

Figure 8: Surface temperature evolution in intermittent downgrinding $T(t, x, 0)$ for $x \in (-\delta, \delta)$ and $t = t^* m/5$, taking $m = 1, 2, 3, 4, 5$ (red, orange, green, blue, magenta, resp.).

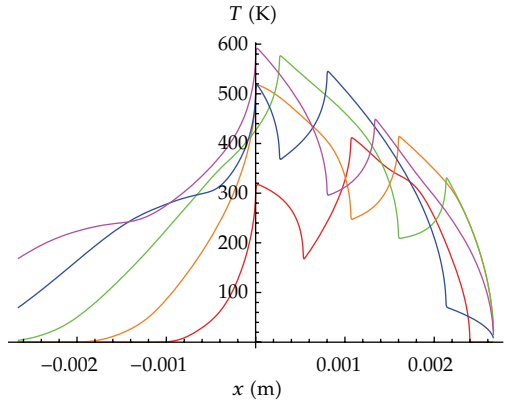

Figure 9: Surface temperature evolution in intermittent upgrinding $T(t, x, 0)$ for $x \in (-\delta, \delta)$ and $t = t^* m/5$, taking $m = 1, 2, 3, 4, 5$ (red, orange, green, blue, magenta, resp.).

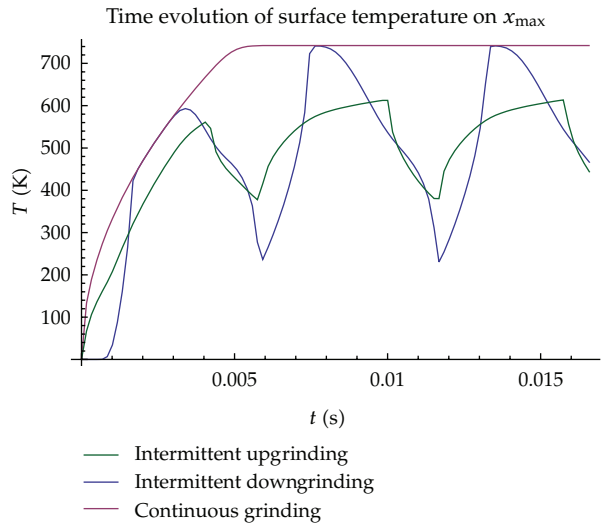

Figure 10: Time evolution of $T_{cont}(t, x_{max}, 0)$ and $T(t, x_{max}, 0)$, for $t \in (0, 2t^*)$.

6. Numerical Analysis

For the plots presented in this section, we have taken as grinding parameters: $\delta = 2.663 \times 10^{-3}$ m, $v_d = 0.53$ m/s, and $q = 5.89 \times 10^7$ W/m^2. We have considered as well a VT20 titanium alloy workpiece, whose thermal properties are $k_0 = 13$ W/(mK) and $k = 4.23 \times 10^{-6}$ m^2/s [16]. Following the procedure described in Section 5.3, the maximum temperature in continuous grinding and its location on the workpiece surface is

$$T_{max} = 742.23\,\text{K}, \qquad x_{max} = 7.1568 \times 10^{-3}\ \delta. \tag{6.1}$$

In order to evaluate the relaxation time, according to (5.38), we have taken a very small parameter $\epsilon = 10^{-6}$ K/s. Taking into account (6.1), we may solve numerically (5.39) and compute the approximation given in (5.43), obtaining

$$t^* = 8.3013 \times 10^{-3}\,\text{s}, \qquad t^* \approx 1.6727 \times 10^{-3}\ s. \tag{6.2}$$

Notice that the results given in (6.2) coincide in order of magnitude.

For the case of intermittent grinding we have taken in (4.1), (4.3), (4.4), and (4.7), the following wheel parameters: $\chi = 0.7\delta$ and $\chi_1 = 0.5\delta$, and a wheel velocity over the workpiece surface $v_m = \delta/t^*$. According to this data, the point period of the quasistationary regime is $\tau = 0.7t^*$, and the global period is $\overline{\tau} = 2.1t^*$. Figures 7, 8, and 9 show the time evolution of the workpiece surface temperature for $t \in (0, t^*)$, for continuous and intermittent up- and downgrinding, respectively. As can be seen, the temporal evolution of up and down grinding is quite different from each other, but in both cases, the continuous profile is a limit boundary. Figure 10 compares the temperature time evolution in x_{max} of continuous grinding with intermittent up- and downgrinding. We may highlight that the relaxation time obtained for the continuous case is a good estimation for the transient regime in the intermittent case. We may notice also how upgrinding nearly saturates the maximum temperature of the

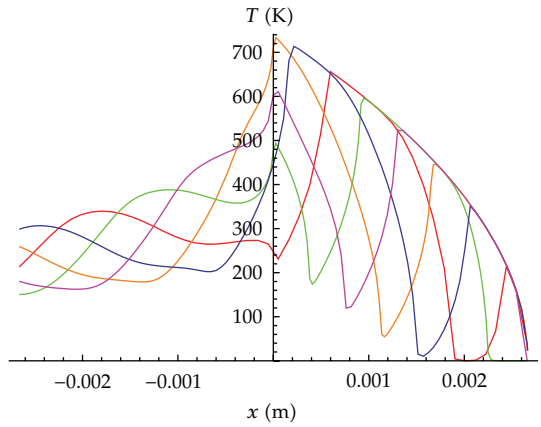

Figure 11: Time evolution of $T_\infty(t, x, y)$ for $x \in (-\delta, \delta)$ and $t = m\overline{\tau}/5$, taking $m = 1, 2, 3, 4, 5$ (red, orange, green, blue, magenta, resp.).

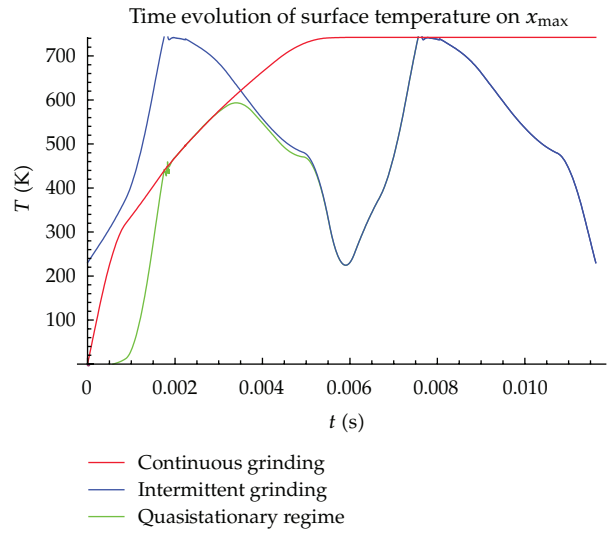

Figure 12: Comparison of the time evolution on $x_{\max}$ for $t \in (0, 2\tau)$.

continuous case, but this does not occur in downgrinding. We may evaluate numerically the maximum temperature, both intermittent up- and downgrindings,

$$T_{\max}^{\text{down}} = 741.41\,\text{K}, \qquad T_{\max}^{\text{up}} = 591.29\,\text{K}. \tag{6.3}$$

Figure 11 shows the time evolution of the quasistationary regime on the surface for a friction period $\overline{\tau}$. For $x < 0$, the temperature oscillates as a wave. This is because the heat flux pulses produced at the contact zone are propagated along the surface just ground. Figure 12 shows the time evolution of the temperature in $x_{\max}$ for $t \in (0, 2\tau)$. On the one hand, we may check that the quasistationary regime has a period τ, as it was commented in (5.9). On the other hand, we may notice that the quasistationary regime is reached when the temperature in the continuous case is saturated. Therefore, the relaxation time t^* defined

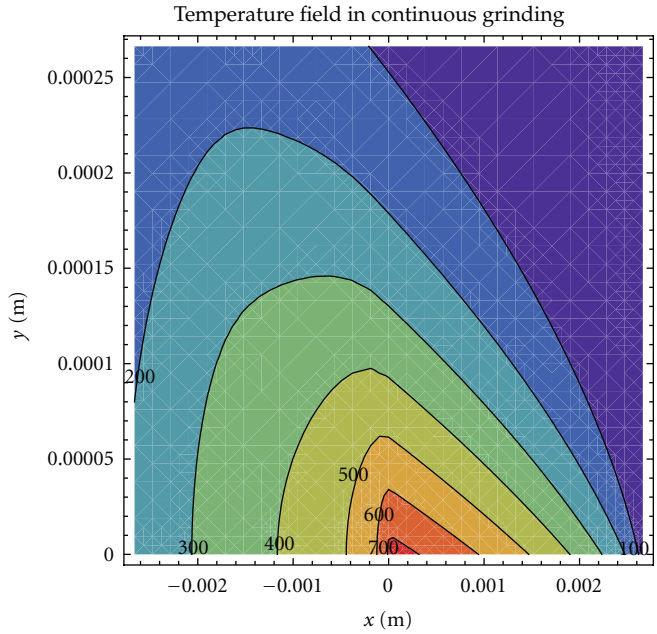

Figure 13: Field temperature $T_{\text{cont}}(t^*, x, y)$ for $(x, y) \in (-\delta, \delta) \times (0, \delta/10)$. Contours give the temperature in K.

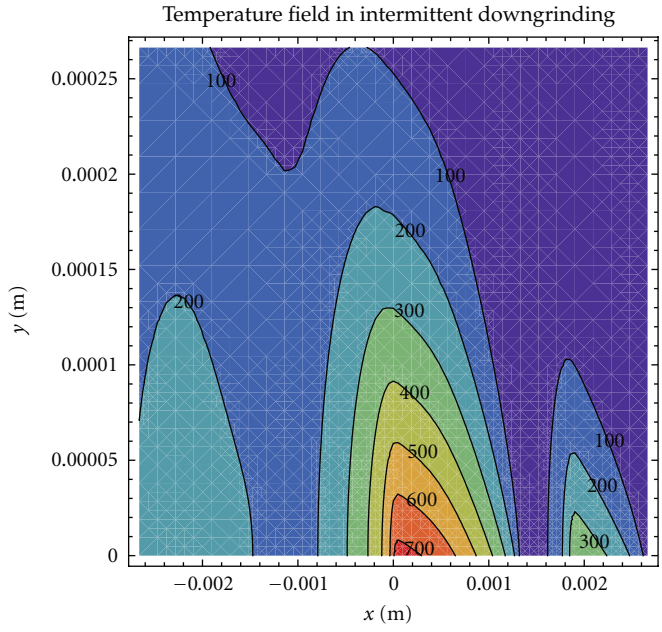

Figure 14: Field temperature $T(t^*, x, y)$ for $(x, y) \in (-\delta, \delta) \times (0, \delta/10)$, in the case of downgrinding. Contours give the temperature in K.

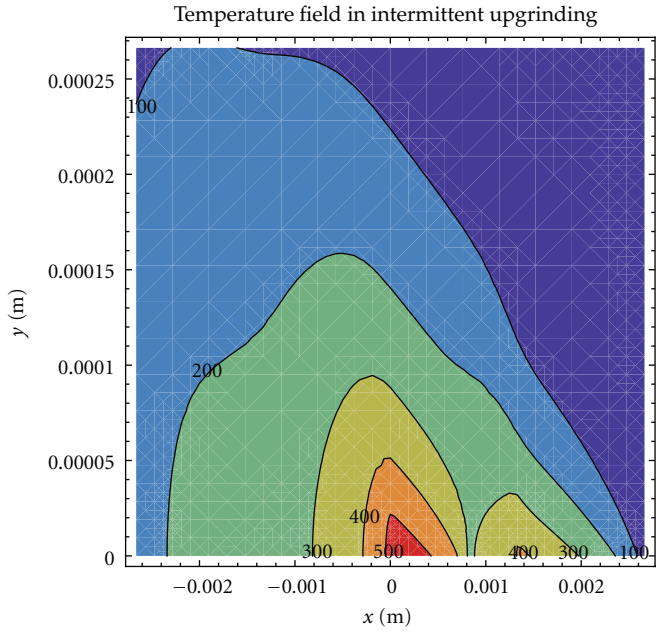

Figure 15: Field temperature $T(t^*, x, y)$ for $(x, y) \in (-\delta, \delta) \times (0, \delta/10)$ in the case of upgrinding. Contours give the temperature in K.

for the continuous case is a good measurement for the transient regime when we have a quasistationary regime in intermittent grinding. In Figures 14 and 15, we have plotted the temperature fields at $t = t^*$, in the cases of up- and downgrinding, respectively. We may realize that both temperature fields are quite different from each other. Figure 13 shows the field temperature for the continuous case. If we compare the temperature field in the continuous case with the intermittent one (up- or downgrinding), we may observe that an intermittent friction distorts the temperature field producing thermic waves inside the workpiece.

7. Conclusions

We have derived a closed analytical solution for the time evolution of the temperature field in dry grinding for any time-dependent friction function. Our result is based on the Samara-Valencia model [9], solving explicitly the evolution of temperature field for the case of dry grinding. We find this solution solving a recurrence equation by successive approximations. We have proved that this solution is unique. An analytical solution of this type has the advantage to be straightforwardly computable, plotting the graphs very rapidly. Also, the dependence of the grinding parameters on the temperature field can be studied. The latter is quite useful for the engineering optimization of the grinding process.

We apply our solution to continuous and intermittent up- and downgrinding. We have tested numerically that the time evolution of up- and downgrinding is quite different from each other. In continuous grinding, we have proved that the maximum temperature occurs at the stationary regime within the friction zone on the surface. In order to graph the evolution of the temperature field, we have obtained a useful approximation for the characteristic time

of the transient regime. Comparing the plots of continuous and intermittent grinding for the same workpiece and grinding parameters, we conclude that the behavior of the intermittent case is more complicated in detail, but in general the magnitude of temperature field is lower. The latter is quite understandable because, in intermittent grinding, the amount of energy per unit time entering into the workpiece due to friction is less than in the continuous case. Therefore, the temperature plot for the continuous grinding acts as a boundary for the intermittent case.

Also, we have tested numerically that the relaxation time obtained for continuous grinding is a good estimation for the characteristic time of the transient regime in the intermittent case. Finally, we have obtained an expression for the quasistationary regime in intermittent grinding, in which the field temperature oscillates periodically.

Acknowledgments

The authors wish to thank the financial support received from *Generalitat Valenciana* under Grant GVA 3012/2009 and from Universidad Politécnica de Valencia under Grant PAID-06-09.

References

[1] S. Malkin, *Grinding Technology: Theory and Applications of Machining with Abrasives*, Ellis Horwood Ltd. and John Wiley and Sons, 1989.

[2] C. Guo and S. Malkin, "Analysis of energy partition in grinding," *Journal of Engineering for Industry*, vol. 117, pp. 55–61, 1995.

[3] S. Malkin and R. B. Anderson, "Thermal aspects of grinding: 1—energy partition," *Journal of Engineering for Industry*, vol. 96, no. 4, pp. 1177–1183, 1974.

[4] A. S. Lavine and B. F. von Turkovich, "Thermal aspects of grinding: the effect of heat generation at the shear planes," *CIRP Annals*, vol. 40, no. 1, pp. 343–345, 1991.

[5] A. S. Lavine, "An exact solution for surface temperature in down grinding," *International Journal of Heat and Mass Transfer*, vol. 43, no. 24, pp. 4447–4456, 2000.

[6] M. Mahdi and Liangchi Zhang, "The finite element thermal analysis of grinding processes by ADINA," *Computers & Structures*, vol. 56, no. 2-3, pp. 313–320, 1995, Proceedings of the 10th ADINA Conference of Nonlinear Finite Element Analysis and ADINA.

[7] A. G. Mamalis, D. E. Manolakos, A. Markopoulos, J. Kundrák, and K. Gyáni, "Thermal modelling of surface grinding using implicit finite element techniques," *International Journal of Advanced Manufacturing Technology*, vol. 21, no. 12, pp. 929–934, 2003.

[8] K. T. Andrews, M. Shillor, and S. Wright, "A model for heat transfer in grinding," *Nonlinear Analysis*, vol. 35, no. 2, pp. 233–246, 1999.

[9] D. L. Skuratov, Yu. L. Ratis, I. A. Selezneva, J. Pérez, P. Fernández de Córdoba, and J. F. Urchueguía, "Mathematical modelling and analytical solution for workpiece temperature in grinding," *Applied Mathematical Modelling*, vol. 31, no. 6, pp. 1039–1047, 2007.

[10] I. S. Gradsthteyn and I. M. Ryzhik, *Table of Integrals, Series and Products*, Academic Press, New York, NY, USA, 7th edition, 2007.

[11] J. L. González-Santander, J. Pérez, P. Fernández de Córdoba, and J. M. Isidro, "An analysis of the temperature field of the workpiece in dry continuous grinding," *Journal of Engineering Mathematics*, vol. 67, no. 3, pp. 165–174, 2010.

[12] J. C. Jaeger, "Moving sources of heat and the temperature at sliding contracts," *The Royal Society of New South Wales*, vol. 76, pp. 204–224, 1942.

[13] M. Abramowitz and I. Stegun, *Handbook of Mathematical Functions*, NBS Applied Mathematics Series 55, NBS, Washington, DC, USA, 1972.

[14] J. L. González-Santander, *Modelización matemática de la transmisión de calor en el proceso del rectificado industrial plano*, Ph.D. thesis, Universidad Politécnica de Valencia, Valencia, Spain, 2009, http://hdl.handle.net/10251/4769.

[15] R. M. Corless, D. J. Jeffrey, and D. E. Knuth, "A sequence of series for the Lambert W function," in *Proceedings of the 1997 International Symposium on Symbolic and Algebraic Computation*, pp. 197–204, ACM Press, Maui, Hawaii, USA, July 1997.

[16] S. G. Glasunov and V. N. Moiseev, *Constructional Titanium Alloys, Metallurgy*, Moscow, Moscow, Russia, 1974.